

Comparison of X-31 Flight and Ground-Based Yawing Moment Asymmetries at High Angles of Attack*

Brent R. Cobleigh

NASA Dryden Flight Research Center
Edwards Air Force Base
P.O. Box 273
D-2028, Edwards, California 93523-0273
USA

Mark A. Croom

NASA Langley Research Center
MS 406, Hampton, AV 23681-2199
USA

ABSTRACT

Significant yawing moment asymmetries were encountered during the high-angle-of-attack envelope expansion of the two X-31 aircraft. These asymmetries caused position saturations of the thrust-vectoring vanes and trailing-edge flaps during some stability-axis rolling maneuvers at high angles of attack. The two test aircraft had different asymmetry characteristics, and ship 2 has asymmetries that vary as a function of Reynolds number. Several aerodynamic modifications have been made to the X-31 forebody with the goal of minimizing the asymmetry. These modifications include adding transition strips on the forebody and noseboom, using two different length strakes, and increasing nose bluntness. Ultimately, a combination of forebody strakes, nose blunting, and noseboom transition strips reduced the yawing moment asymmetry enough to fully expand the high-angle-of-attack envelope. Analysis of the X-31 flight data is reviewed and compared to wind-tunnel and water-tunnel measurements. Several lessons learned are outlined regarding high-angle-of-attack configuration design and ground testing.

NOMENCLATURE

C_d	cylinder drag coefficient
C_n	yawing moment coefficient
C_{n_0}	yawing moment coefficient at 0° angle of sideslip
C_Y	side force coefficient
$ C_Y _{max}$	maximum absolute value of the side force coefficient
d	noseboom diameter
D	forebody or ogive base diameter
g	acceleration caused by gravity
l	body length
Re_D	Reynolds number based on a forebody base diameter of 3.2 ft (97.5 cm)
Re_d	Reynolds number based on a noseboom diameter of 3.5 in. (8.9 cm)
S1	strake 20-in. (50.8-cm) long by 0.60-in. (1.52-cm) wide
S2	strake 47-in. (119.4-cm) long by 0.60-in. (1.52-cm) wide
V	velocity
α	angle of attack, deg

* Notice: Use of trade names or names of manufacturers in this document does not constitute an official endorsement of such products or manufacturers, either expressed or implied, by the National Aeronautics and Space Administration.

Report Documentation Page				Form Approved OMB No. 0704-0188	
Public reporting burden for the collection of information is estimated to average 1 hour per response, including the time for reviewing instructions, searching existing data sources, gathering and maintaining the data needed, and completing and reviewing the collection of information. Send comments regarding this burden estimate or any other aspect of this collection of information, including suggestions for reducing this burden, to Washington Headquarters Services, Directorate for Information Operations and Reports, 1215 Jefferson Davis Highway, Suite 1204, Arlington VA 22202-4302. Respondents should be aware that notwithstanding any other provision of law, no person shall be subject to a penalty for failing to comply with a collection of information if it does not display a currently valid OMB control number.					
1. REPORT DATE 00 MAR 2003		2. REPORT TYPE N/A		3. DATES COVERED -	
4. TITLE AND SUBTITLE Comparison of X-31 Flight and Ground-Based Yawing Moment Asymmetries at High Angles of Attack				5a. CONTRACT NUMBER	
				5b. GRANT NUMBER	
				5c. PROGRAM ELEMENT NUMBER	
6. AUTHOR(S)				5d. PROJECT NUMBER	
				5e. TASK NUMBER	
				5f. WORK UNIT NUMBER	
7. PERFORMING ORGANIZATION NAME(S) AND ADDRESS(ES) NATO Research and Technology Organisation BP 25, 7 Rue Ancelle, F-92201 Neuilly-Sue-Seine Cedex, France				8. PERFORMING ORGANIZATION REPORT NUMBER	
9. SPONSORING/MONITORING AGENCY NAME(S) AND ADDRESS(ES)				10. SPONSOR/MONITOR'S ACRONYM(S)	
				11. SPONSOR/MONITOR'S REPORT NUMBER(S)	
12. DISTRIBUTION/AVAILABILITY STATEMENT Approved for public release, distribution unlimited					
13. SUPPLEMENTARY NOTES Also see: ADM001490, Presented at RTO Applied Vehicle Technology Panel (AVT) Symposium held inLeon, Norway on 7-11 May 2001, The original document contains color images.					
14. ABSTRACT					
15. SUBJECT TERMS					
16. SECURITY CLASSIFICATION OF:			17. LIMITATION OF ABSTRACT UU	18. NUMBER OF PAGES 14	19a. NAME OF RESPONSIBLE PERSON
a. REPORT unclassified	b. ABSTRACT unclassified	c. THIS PAGE unclassified			

INTRODUCTION

Two X-31 aircraft (fig. 1) were designed and built to support the Enhanced Fighter Maneuverability (EFM) research program,¹ which was jointly funded by the United States Defense Advanced Research Projects Agency (DARPA) and the German Federal Ministry of Defense. The flight test portion of the program was conducted by an international test organization composed of the National Aeronautics and Space Administration (NASA), the U. S. Navy, the U. S. Air Force, Rockwell International (Downey, California), and Deutsche Aerospace (DASA). The goals of the flight program were to demonstrate enhanced fighter maneuverability technologies, investigate close-in-combat exchange ratios, develop design requirements, build a database for application to future fighter aircraft, and develop and validate low-cost prototype concepts.

During the 1-g, high-angle-of-attack envelope expansion, both X-31 test aircraft exhibited significant, but different, yawing moment asymmetries at 0° angle of sideslip at angles of attack greater than 40°. Resulting aircraft responses included slow rollovers and “lurches” (small, sharp, heading changes). Although pilot compensation was attainable, as much as 50 percent of roll-stick deflection was required to counter the asymmetry. Consequently, the full-stick velocity vector roll rate of each aircraft was found to be faster in the direction of the asymmetry at a constant angle of attack. To coordinate maneuvering with the yawing moment asymmetries, the control system had to increase the amount of control deflection required. In many cases, this increase resulted in a position saturation of one of the trailing-edge flaps or thrust-vectoring paddles.

In an attempt to reduce the yawing moment asymmetry, transition grit strips were applied along the forebody to force boundary-layer transition at the same location on both sides of the forebody. This method had shown some promise in reducing high-angle-of-attack yawing asymmetries during earlier tests on the F-18 High Alpha Research Vehicle (HARV).² Transition strips were also installed along the noseboom with the hopes that a turbulent separation from the cylindrical cross section would result in a reduced wake impinging on the forebody. These configuration changes somewhat improved the pilot-reported handling qualities; however, the asymmetries were not eliminated.

Shortly into the high-angle-of-attack, elevated-g phase of the envelope expansion, a departure from controlled flight occurred on ship 2 as the pilot was performing a 2-g, split-S maneuver to 60° angle of attack. Data analysis showed that a large, unmodeled yawing moment, in excess of the available control power, had triggered the departure. The forebody vortex system was suspected to be the moment generator.

An effort was begun to design and test forebody strakes that would improve the forebody vortex symmetry and eliminate any large-amplitude asymmetry changes like those seen during the departure. Towards this goal, a wind-tunnel test³ was conducted in the NASA Langley Research Center (Hampton, Virginia) 30- by 60-Foot Wind Tunnel to define the strake design and document any changes to the static stability characteristics. The test resulted in the installation and flight test of small forebody strakes that ultimately reduced the asymmetry enough to fully achieve all of the flight test objectives. Shortly after the strake design, a water-tunnel test⁴ was conducted in the NASA Dryden Flight Research Center (Edwards, California) Flow Visualization Facility to investigate the variation in forebody flow characteristics as a function of configuration changes.

This report summarizes the effectiveness of the configuration modifications that were flight-tested and the usefulness of the ground test facilities at predicting the X-31 forebody aerodynamics. The lessons learned during the X-31 program illustrate the sensitivity of forebody aerodynamics to Reynolds number and seemingly minor configuration changes.

FOREBODY AERODYNAMICS BACKGROUND

The long, slender, forebody shapes of modern fighter aircraft make them susceptible to the forebody side force phenomenon. This side force is the result of surface pressure imbalances around the forebody caused by an asymmetric forebody boundary-layer separation and vortex system at high angles of attack. In this scenario, the boundary layer on each side of the forebody separates at different locations as shown in the forebody cross section in figure 2. At separation, corresponding vortex sheets are generated that roll into an

asymmetrically positioned vortex pair. The forces on the forebody are primarily generated by the attached flow and to a lesser extent by the vortices, depending on their proximity to the forebody surface. Figure 2 shows a typical asymmetrical arrangement in which the lower, more inboard vortex corresponds to a boundary layer that separated later and the higher, more outboard vortex corresponds to the boundary layer that separated earlier. The suction generated by the longer run of attached flow and the closer vortex combine to create a net force in that direction. Because the aircraft center of gravity is well aft of the forebody, a sizable yawing moment asymmetry develops.

The asymmetry problem was illustrated by measuring the side force on an axisymmetric body at different roll angles and angles of attack. Because the model is axisymmetric, no lateral-directional forces or moments would be expected. Figure 3, however, shows that a large asymmetry develops on a $3.5\text{-}l/D$ fineness-ratio ogive model at approximately 35° and continues to greater than 70° angle of attack.⁵ In addition, as the ogive is rotated around its axis of symmetry, the sign of the asymmetry changes at a roll angle of 270° . Further tests by other researchers confirmed that the magnitude of the asymmetry does not change smoothly with changing roll angle⁶⁻⁸ (fig. 4). Instead, as the ogive cylinder is rolled through 360° , four changes in the sign of the asymmetry occur. Thus, at high angles of attack, the vortex cores can have bistable states, neither of which is symmetric. Other tests have shown that rotation of the nosetip alone produces the same result, suggesting that microasymmetries near the model tip are significant in the asymmetry formation.^{5, 7, 9-11}

Reynolds number also has been shown to affect the asymmetry characteristic of slender bodies.^{5, 6, 9, 12} Figure 5 shows that large changes in the magnitude and sign of the asymmetry can be affected by Reynolds number; however, the angle-of-attack range over which the aircraft is susceptible to asymmetries remains unchanged. The nature of the boundary-layer separation on the forebody—whether it is laminar, transitional, or fully turbulent—depends on the Reynolds number. At angles of attack greater than 30° , the maximum side force on a $3.5\text{-}l/D$ ogive is significantly larger for laminar and turbulent separation conditions than it is with transitional flow (fig. 6). This Reynolds number effect is important when comparing flight-derived asymmetry information with either wind-tunnel or water-tunnel data.

Several methods have been used to reduce the asymmetry characteristics of high-angle-of-attack aircraft. The traditional passive method of controlling the forebody vortex location has been to use longitudinal strakes near the apex on both sides of the forebody. Techniques that address the boundary-layer state have also gained attention. Because the nosetip appears to have a large influence on the asymmetry, several modifications to it also have been studied.^{5, 7, 9-11}

Strakes have been shown to reduce or eliminate high-angle-of-attack side force asymmetries on generic cone and ogive shapes^{9, 13} and realistic aircraft forebodies.¹⁴⁻¹⁷ Cases of strakes not fully eliminating the asymmetry have also been found.¹⁸ The addition of strakes near the nosetip produces several beneficial effects on the forebody flow field. First, the strakes tend to mask the presence of microasymmetries on the model or aircraft. Second, the strakes fix the boundary-layer separation line on the body, eliminating asymmetric boundary-layer separation as a cause of vortex asymmetry. Last, the strakes increase the vorticity (and thus the strength) of the primary vortex cores, making them less susceptible to other flow fields such as the canard or wing.

Boundary-layer transition, or “trip,” strips also have had limited success at reducing asymmetries. One use of transition strips is to ensure the boundary layer transitions to a turbulent state symmetrically on both sides of the forebody. Having similar boundary-layer states should promote symmetrical separation and vortex formation. In limited tests on the HARV,² a symmetrically applied transition grit strip eliminated the asymmetric separation caused by asymmetric vortices. Excellent reviews of the high-angle-of-attack vortex asymmetry problem have been compiled by Hunt¹⁹ and Ericsson.²⁰

FLIGHT TEST RESULTS

Flight data were recorded during the high-angle-of-attack envelope expansion of the two X-31 aircraft. Additional analysis of the X-31 yawing moment asymmetry flight data is discussed in references 21 and 22.

Method

To better understand and quantify the high-angle-of-attack yawing moment asymmetry characteristic of the X-31 aircraft, a method has been developed to calculate time histories of the asymmetric forces and moments on the aircraft from flight data. Figure 7 shows a block diagram of the method. The flight-measured yawing moment is computed by substituting the measured variables into the rigid-body equation of motion. The yawing moment predicted from the simulation aerodynamic and thrust databases is then subtracted from the flight-measured moment to calculate the missing, unmodeled components.

By restricting data analysis to symmetrical maneuvers in which sideslip, roll rate, and yaw rate are small, the cause of the missing aerodynamic yawing moment has been narrowed to three main sources: errors in the thrust-vectoring model; errors in the control effectiveness model; and aerodynamic asymmetries. Because the control effectiveness database was verified and updated with parameter identification results and the thrust model errors were not expected to be a strong function of angle of attack, any changes in the missing components with increases in angle of attack were attributed to aerodynamic asymmetries. An analysis of multiple decelerations, pullups, and split-S maneuvers with the same aircraft configuration resulted in a composite of the asymmetry characteristic for the given configuration at a given flight condition.

Maneuver Technique

The X-31 control laws were designed to allow the pilot to command angle of attack with the pitch stick, stability-axis roll rate with the roll stick, and angle of sideslip with the rudder pedals. The angle-of-sideslip commands were faded to 0° between 30° and 50° angle of attack. Two control-law features made the maneuvers shown herein nearly independent of pilot technique. One of these features was an angle-of-attack limiter. The angle-of-attack limiter allowed the pilot to set the maximum angle-of-attack command that the control laws would generate for a specific maneuver, which permitted the pilot to pull the stick aft of the target command, resulting in an angle-of-attack command that stopped at the limiter setting. The other feature was a 25-deg/sec rate limiter on the angle-of-attack command. Thus, when the pilot pulled the stick quickly aft to the stop, the angle-of-attack command would ramp in to the preselected angle-of-attack limit and remain constant until the pilot released the stick. This technique resulted in nearly identical control system commands for each of the dynamic maneuvers.

Flight Test Configurations

The X-31 forebody is elliptical in cross section with an l/D ratio of approximately 2.2. The aircraft was always flown with an underslung noseboom (fig. 8). The bluntness of the nosetip (nometip radius divided by forebody base radius) was 0.003 in its unmodified configuration. During the course of the study, the following configuration changes were tested (fig. 8):

- S1, a strake 20-in. (50.8-cm) long by 0.60-in. (1.52-cm) wide with nosetip blunting
- S2, a strake 47-in. (119.4-cm) long by 0.60-in. (1.52-cm) wide with nosetip blunting
- Forebody transition strip
- Noseboom transition strip

Whenever the vehicles were flown with a strake, the radius of the nosetip was increased. On ship 1, the nosetip radius was increased to 0.75 in. (0.039 nosetip bluntness). On ship 2, the radius was increased to 0.50 in. (0.026 nosetip bluntness). The transition strips consisted of number 30 Carborundum™ (Saint Gobain Industrial Ceramics; Amherst, Massachusetts) grit. Because the objective was to rapidly alleviate the asymmetry problem, these configuration modifications were not systematically evaluated. The sequence of test configurations was as follows:

Ship 1	Ship 2
Unmodified forebody	Unmodified forebody
Forebody and noseboom transition strips	Forebody and noseboom transition strips
S1 and noseboom transition strip	Forebody transition strip
S1 and forebody and noseboom transition strips	S1 and noseboom transition strip
S1 and noseboom transition strip	S2 and noseboom transition strip

Ship 1 Asymmetries

Figure 9 shows the yawing moment asymmetry for the X-31 ship 1 during slow (approximately 1-g) decelerations to high-angle-of-attack conditions for several of the flight configurations. The largest asymmetry began building up at 48° angle of attack and had a peak yawing moment asymmetry of $C_{n_0} = -0.063$ at approximately 57° angle of attack. The asymmetry diminished significantly in magnitude by 65° angle of attack.

To mitigate these asymmetries, a transition grit strip was installed on both sides of the forebody and along the sides of the noseboom. Unfortunately, the data (fig. 9) indicate that the asymmetry problem was magnified. Although the largest asymmetry began to build at the same angle of attack (48°), the peak asymmetry increased to $C_{n_0} = -0.078$. The addition of the transition strips increased the angle of attack at which the largest asymmetry occurred from 57° to 61°.

The replacement of the forebody transition strip with the S1 strake, combined with the blunting of the nosetip, effectively delayed the initiation of the yawing moment asymmetry to a maximum of 55° angle of attack. A peak asymmetry of $C_{n_0} = -0.040$ occurred at 60° angle of attack, after which the asymmetry diminished. As with the unmodified forebody, the aircraft became nearly symmetric by 65° angle of attack.

The addition of a boundary-layer transition strip along the forebody aft of the strake resulted in an increase in the asymmetry level. A sharp change in the asymmetry occurred at approximately 55° angle of attack. An asymmetry level of $C_{n_0} = -0.050$ remained over an angle-of-attack range from 59° to 66°. Thus, the addition of the forebody transition strip increased the yawing moment asymmetry and caused it to remain at its largest level for a broader angle-of-attack range.

Ship 2 Asymmetries

The yawing moment asymmetry characteristic of ship 2 was significantly more troublesome than that of ship 1; thus, greater effort was made to reduce the asymmetry on ship 2 through configuration changes. In addition to the configuration changes flown with ship 1, the extended-length strake, S2, was also tested.

Unlike ship 1, a comparison of multiple 1-g maneuvers using the unmodified forebody did not show a repeatable trend in the asymmetry as angle of attack increased. Each maneuver appeared to have a random asymmetry pattern. Plots of the asymmetry range as a function of angle of attack (fig. 10) show that the maximum yawing moment asymmetry appears to be bounded at $|C_{n_0}| < 0.10$.

The addition of forebody and noseboom transition strips resulted in a more repeatable asymmetry characteristic than that for the unmodified forebody during 1-g decelerations; however, some scatter still existed about the average asymmetry. Figure 11 shows the range of the scatter for this configuration. The asymmetry initially went to the right to a peak of a maximum of $C_{n_0} = 0.050$ at an angle of attack between 48° and 54°. As the angle of attack increased, the asymmetry switched to the left, eventually reaching its maximum asymmetry at approximately 67° angle of attack. The switching of the asymmetry from the right to left resulted in a change in the yawing moment of between 0.10 and 0.14.

Figure 11 also shows that two different asymmetry characteristics developed on ship 2 when the noseboom transition strip was removed, leaving the forebody transition strip in place. Calculating the approximate crossflow Reynolds number based on noseboom diameter for each of the maneuvers shows that the two asymmetry characteristics occurred over distinct Reynolds number ranges. Plotting both Reynolds number ranges on a chart of the boundary-layer separation state of a circular cylinder as a function of Reynolds number (fig. 12) shows that a difference in the boundary-layer state at separation could have existed between the two sets of data. The lower Reynolds number data, which would result in a large separation wake, had a sharp change in the asymmetry at angles of attack greater than 50° that built up to a large right asymmetry. Conversely, the higher Reynolds number flow, which would produce a smaller separation wake, had a milder buildup in asymmetry. The higher Reynolds number data more closely matched the data with the noseboom transition strips installed, suggesting that the strip was successful in eliminating a laminar separation, as it was originally intended to do.

The first real improvement in the yawing moment asymmetries on ship 2 was found with the addition of forebody strakes and the blunting of the nosetip. Figure 13 shows data from the S1 and S2 strake flight tests. The combination of the S1 strake, 0.5-in.-radius blunt nosetip, and noseboom transition strip resulted in a comparably slow buildup of asymmetry starting at approximately 50° angle of attack. The asymmetry reached a peak value of $C_{n_0} = -0.059$ at 60° angle of attack. As with most other configurations, the asymmetry diminished to nearly zero by 70° angle of attack. The addition of a transition strip aft of the S1 strake increased the maximum asymmetry from $C_{n_0} = -0.059$ to $C_{n_0} = -0.078$. This increase was similar to that seen on ship 1. Because the 20-in.-long S1 strake reduced the maximum yawing moment asymmetry level, a longer 46-in. strake, S2, was installed and flight-tested with the blunt nosetip. Unfortunately, little change in the 1-g deceleration asymmetries resulted. The longer strake did shift the asymmetry to a higher angle of attack by approximately 2°.

Dynamic High-Angle-of-Attack Maneuvers

Figure 14 shows the asymmetries calculated during rapid pullups to high angles of attack for ship 1 for the configuration that had the S1 strake, blunted nose, and noseboom transition strip. The data obtained from the 1-g, quasi-steady-state decelerations are plotted with the dynamic data for comparison. The asymmetry level during the dynamic maneuvers generally was less than or equal to the value seen in the 1-g maneuvers at the maximum asymmetry angle of attack (approximately 60°). This reduction in asymmetry level during the dynamic portion of the maneuver, however, was not entirely useful. As the aircraft reached its target angle of attack and the load factor decayed to unity, the asymmetry often built up to the steady-state value. Thus, the maximum asymmetry defined by the 1-g decelerations provided the “worst-case” levels for which the flight control system had to account. Although the dynamic maneuvers reduced the maximum asymmetry at approximately 60° angle of attack, an increase in the asymmetry was seen at lower angles of attack (approximately 45°–50°).

Similar results were found for ship 2, except that the maximum asymmetry measured when capturing 50° angle of attack increased with increasing Reynolds number (fig. 15). Although the addition of the S2 strake did not appear to reduce the maximum asymmetry at 60° angle of attack, the tendency of the asymmetry to go right at 50° angle of attack during dynamic maneuvers appeared to be significantly reduced.

COMPARISON TO WIND-TUNNEL RESULTS

Shortly after the yawing moment-induced, high-angle-of-attack departure of the X-31 ship 2, a wind-tunnel test³ was conducted in the NASA Langley 30- by 60-Foot Wind Tunnel. The goal of the wind-tunnel test was to aid design of a simple forebody modification that would reduce the high-angle-of-attack yawing moment asymmetry to allow completion of the high-angle-of-attack envelope expansion.

Although some yawing moment asymmetry was predicted in the wind tunnel at the high-angle-of-attack condition, the magnitude was significantly less than that seen in flight (fig. 16). One possible explanation has to do with Reynolds number. A plot of the asymmetry as a function of Reynolds number for an ogive (fig. 6) shows a significant decrease in the asymmetry at Reynolds numbers that result in mixed boundary-layer states on the forebody. The boundary layers that are dominated by laminar or turbulent flow result in similar, large-amplitude asymmetries. If this phenomenon holds true for realistic forebodies in flight, then the Reynolds number of the 30- by 60-Foot Wind Tunnel test could have been responsible for the failure to predict the large amplitude asymmetry. Both the water-tunnel and the flight test Reynolds numbers appear to be well outside of this Reynolds number range.

The wind-tunnel test showed that strakes running longitudinally along the waterline of the forebody from the nosetip reduced the model yawing moment asymmetry. The effectiveness of the strakes at reducing the asymmetry was not a function of the strake width. As previously shown, two different length strake sets were flight-tested and evaluated. Two strake designs, 20-in. (50.8-cm) and 47-in. (119.4-cm) long, were manufactured and flight-tested in separate tests. Both strakes were 0.60-in. (1.52-cm) wide.

The wind-tunnel test was also used to predict the changes to the basic aircraft static aerodynamics caused by the strakes. These predictions were important because several of the candidate strake designs caused undesirable changes to the yawing moment caused by angle of sideslip or the static pitching moment. As an

example, the S2 stakes produced a noseup pitching moment increment over the S1 strakes. When the field of candidate strakes was reduced, the impact of the strake on the overall flying qualities under realistic dynamic conditions was evaluated using the NASA Langley “drop model” technique.³ Using these scale-model test methods resulted in rapid acceptance of the final strake design taken to flight.

To determine what level of asymmetry could be generated on the X-31 forebody in the wind tunnel, a test was run with a strake only on one side of the forebody. A comparison of the asymmetry measured with the one-sided strake to the maximum asymmetry measured in flight with no strake shows a reasonably good comparison (fig. 17), both of magnitude and range. The yawing moment asymmetry magnitude was slightly larger with the one-sided strake than it was in the flight data. Thus, using a small strake to force asymmetric boundary-layer separation resulted in data that more closely matched that measured in flight. This method potentially can simulate a Reynolds number approximating flight conditions to get better estimates of the worst-case vortex-induced asymmetries. These estimates then could be used to define control power requirements and aid in control-law design.

COMPARISON TO WATER-TUNNEL RESULTS

Shortly before the first flight with the new forebody strakes, a water-tunnel test of a 4.4-percent-scale forebody-only model of the X-31 was conducted at the NASA Dryden Flow Visualization Facility.⁴ The study primarily focused on determining the relative effects of the different forebody configurations on the stability and symmetry of the high-angle-of-attack vortex flow field. No force-balance data were obtained, but extensive flow visualization was conducted.

Although no quantitative data were taken, the water-tunnel flow visualization results were reasonably consistent with the flight data. Asymmetries in the boundary-layer separation and vortex core locations were seen between 50° and 65° angle of attack, as they were in the flight results. The largest deviation between the left and right vortex and boundary-layer positions was seen at 60° angle of attack (fig. 18), which correlates with the angle of the greatest asymmetry magnitude in flight. The water-tunnel model also showed a change in the sign of the asymmetry as the angle of attack increased from 55° to 60°. This change in asymmetry sign was similar to that measured on ship 2 (figs. 10 and 11) over the same angle-of-attack range in flight.

The installation of the strakes on the model increased the vorticity in the vortex cores, but did not eliminate the asymmetry. Flight results also showed that the strakes did not fully eliminate the asymmetry.

Tests without the noseboom installed were also completed. Surprisingly, no asymmetries were found at any angle of attack, regardless of the strake configuration. In the water tunnel, the unsteady wake of the noseboom appeared to be the catalyst that triggered the asymmetries to form. This oscillating wake initiated at approximately 50° angle of attack. An alternative L-shaped noseboom—whose wake did not intersect the critical, forward portion of the forebody—did not produce asymmetries in the vortex cores.⁴ A nosetip boom similar to the X-29 noseboom failed to eliminate the forebody vortex system asymmetry.⁴ Whether or not these alternative noseboom configurations would have similar effects on the full-scale aircraft could not be determined.

LESSONS LEARNED

Several lessons learned during the X-31 program should be considered when designing and testing a high-angle-of-attack aircraft. First, caution must be used during high-angle-of-attack wind-tunnel entries when testing configurations or components that are near the critical Reynolds number range. Whenever possible, testing should be accomplished over a range of Reynolds numbers to determine the sensitivity of the configuration to Reynolds number.

Second, during the X-31 wind-tunnel evaluation, an asymmetric strake configuration yielded yawing moment predictions at approximately the flight-measured values. This technique is suggested as an easy method to assess the worst-case yawing moment asymmetry that could develop.

Third, flight analysis and ground testing has shown that the X-31 noseboom played a role in the character of the yawing moment asymmetry. Whether this role was affecting the asymmetry magnitude and changes with angle of attack or, as was suggested by water-tunnel testing, acting as the trigger for the asymmetric flow

remains unclear. Regardless, noseboom configurations are frequently problematic for high-angle-of-attack vehicles.

CONCLUSIONS

An analysis of the yawing moment asymmetry of the X-31 aircraft from static and dynamic flight data was completed for the basic and several modified forebody configurations. The two test aircraft were found to have different asymmetry characteristics, although no significant geometric differences were found.

Transition strips applied along the forebody in an attempt to produce a symmetrical boundary-layer state and separation line resulted in an increase in the X-31 yawing moment asymmetry. Similar transition strips applied along the underslung, cylindrical noseboom made the Reynolds number-sensitive asymmetry characteristic more repeatable on ship 2.

The combination of small strakes installed near the nosetip and increased nosetip radius reduced the yawing moment asymmetry magnitude on both aircraft. In addition, the asymmetry initiated at a higher angle of attack and was characterized by a more repeatable pattern with increasing angle of attack.

REFERENCES

¹Alcorn, C. W., M. A. Croom, M. S. Francis, and H. Ross, "The X-31 Aircraft: Advances in Aircraft Agility and Performance," *Progress in Aerospace Sciences*, vol. 32, no. 4, pp. 377–413, Aug. 1996.

²Fisher, David F. and Brent R. Cobleigh, "Controlling Forebody Asymmetries In-Flight-Experience with Boundary Layer Transition Strips," AIAA-94-1826, June 1994.

³Croom, Mark A., David J. Fratello, Raymond D. Whipple, Matthew J. O'Rourke, and Todd W. Trilling, "Dynamic Model Testing of the X-31 Configuration for High Angle of Attack Flight Dynamics Research," AIAA-93-3674-CP, Aug. 1993.

⁴Cobleigh, Brent and John Del Frate, *Water Tunnel Flow Visualization Study of a 4.4% Scale X-31 Forebody*, NASA TM-104276, 1994.

⁵Keener, Earl P., Gary T. Chapman, Lee Cohen, and Jamshid Taleghani, *Side Forces on a Tangent Ogive Forebody with a Fineness Ratio of 3.5 at High Angles of Attack and Mach Numbers from .1 to .7*, NASA TM-X-3437, 1977.

⁶Lamont, P. J., "Pressure Measurements on an Ogive-Cylinder at High Angles of Attack with Laminar, Transitional, or Turbulent Separation," AIAA-80-1556, Jan. 1980.

⁷Moskovitz, C., R. Hall, and F. DeJarnette, "Experimental Investigation of a New Device to Control the Asymmetric Flowfield on Forebodies at Large Angles of Attack," AIAA-90-0069, Jan. 1990.

⁸Bridges, David H. and Hans G. Hornung, "Elliptic Cross Section Tip Effects on the Vortex Wake of an Axisymmetric Body at High Angle of Attack," AIAA-93-2960, July 1993.

⁹Chapman G. T., E. R. Keener, and G. N. Malcolm, "Asymmetric Aerodynamic Forces on Aircraft Forebodies at High Angle of Attack - Some Design Guides," AGARD-CP-199, Nov. 1975.

¹⁰Kruse, Robert L., Earl R. Keener, Gary T. Chapman, and Gary Claser, *Investigation of the Asymmetric Aerodynamic Characteristics of Cylindrical Bodies of Revolution With Variations in Nose Geometry and Rotational Orientation at Angles of Attack to 58° and Mach Numbers to 2*, NASA TM-78533, 1979.

¹¹Moskovitz, Cary A., Robert M. Hall, and F. R. DeJarnette, "Effects of Nose Bluntness, Roughness and Surface Perturbations on the Asymmetric Flow Past Slender Bodies at Large Angles of Attack," AIAA-89-2236-CP, 1989.

¹²Lamont, P. J., "The Complex Asymmetric Flow Over a 3.5D Ogive Nose and Cylindrical Afterbody at High Angles of Attack," AIAA-82-0053, Jan. 1982.

¹³Fisher, David F., David M. Richwine, and Stephen Landers, *Correlation of Forebody Pressures and Aircraft Yawing Moments on the X-29A Aircraft at High Angles of Attack*, NASA TM-4417, 1992.

¹⁴Skow, A. M. and G. E. Ericsson, "Modern Fighter Aircraft Design for High-Angle-of-Attack Maneuvering," AGARD-LS-121, Mar. 1982, pp. 4-1-4-59.

¹⁵Coe, Paul L., Jr., Joseph R. Chambers, and William Letko, *Asymmetrical Lateral-Directional Characteristics of Pointed Bodies of Revolution at High Angles of Attack*, NASA TN-D-7095, 1972.

¹⁶Malcolm, Gerald N. and T. T. Ng, "Aerodynamic Control of Aircraft by Forebody Vortex Manipulation," AIAA-90-1827, Feb. 1990.

¹⁷Ng, T. T. and G. N. Malcolm, "Aerodynamic Control Using Forebody Strakes," AIAA-91-0618, Jan. 1991.

¹⁸Hassell, James L., Jr. and Donald E. Hewes, *Investigation of the Subsonic Stability and Control Characteristics of a 1/7-Scale Model of the North American X-15 Airplane With and Without Fuselage Forebody Strakes*, NASA TM-X-210, 1960.

¹⁹Hunt, B. L., "Asymmetric Vortex Forces and Wakes on Slender Bodies," AIAA-82-1336, Aug. 1982.

²⁰Ericsson, L. E., "Control of Forebody Flow Asymmetry - A Critical Review," AIAA-90-2833-CP, 1990.

²¹Cobleigh, Brent R., *High-Angle-of-Attack Yawing Moment Asymmetry of the X-31 Aircraft from Flight Test*, NASA CR-186030, 1994

²²Fisher, David F., Brent R. Cobleigh, Daniel W. Banks, Robert M. Hall, and Richard W. Wahls, *Reynold's Number Effects at High Angles of Attack*, NASA TP-1998-206553, 1998.

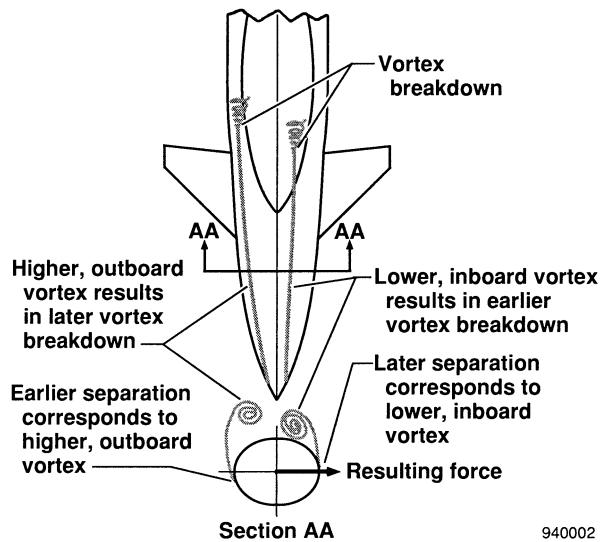
²³Shevell, Richard S., *Fundamentals of Flight*, Prentice-Hall Inc., Englewood Cliffs, New Jersey, 1983.

FIGURES



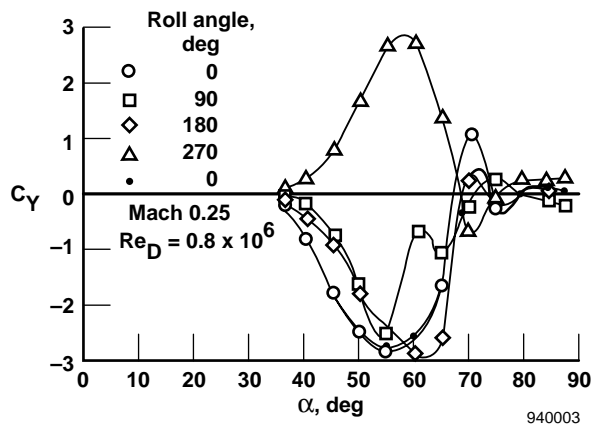
EC92-04233-9

Figure 1. The X-31 aircraft in flight.

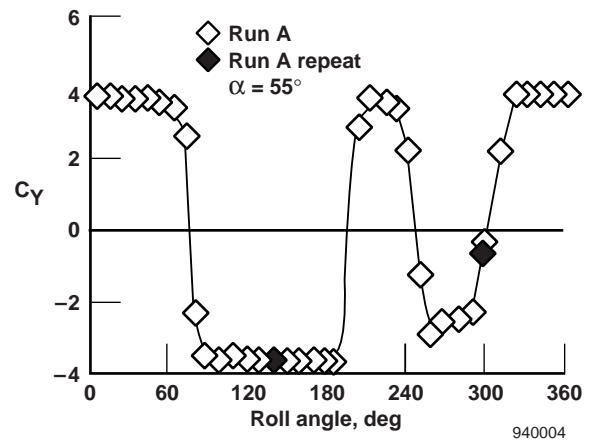


940002

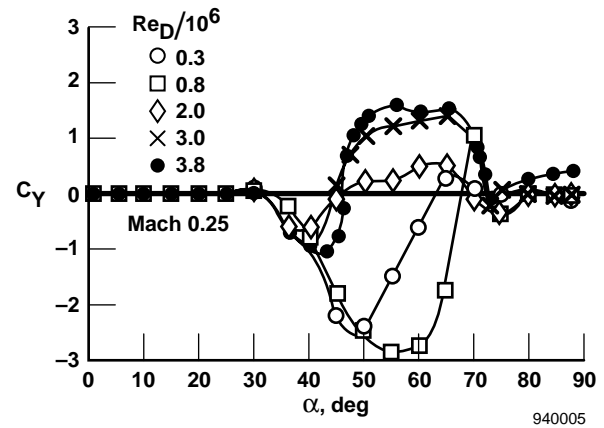
Figure 2. Asymmetrical forebody vortex system.



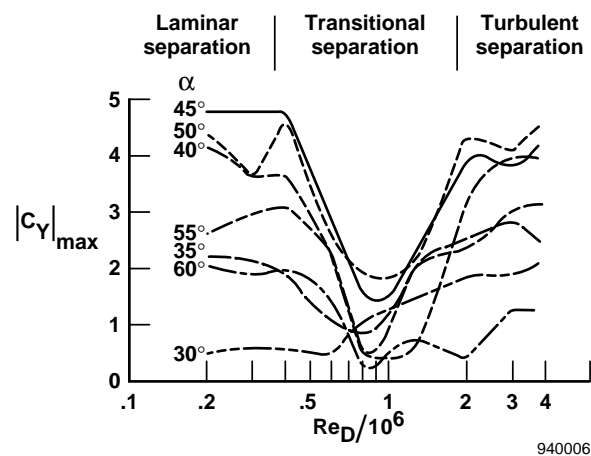
940003

Figure 3. Side force asymmetry of a 3.5-l/D ogive as a function of angle of attack.⁵

940004

Figure 4. Variation of side force coefficient on a 3.0-l/D ogive cylinder with model roll angle.⁶

940005

Figure 5. Effect of Reynolds number on the side force of a 3.5-l/D ogive.⁵

940006

Figure 6. Variation of maximum side force on a 3.5-l/D ogive with Reynolds number for several angles of attack.¹²

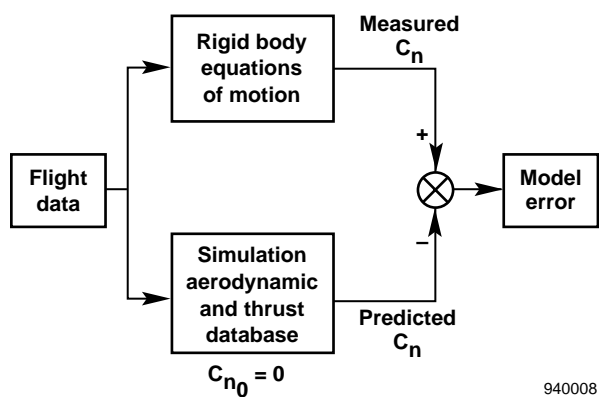


Figure 7. Determination of unmodeled asymmetries from flight data.

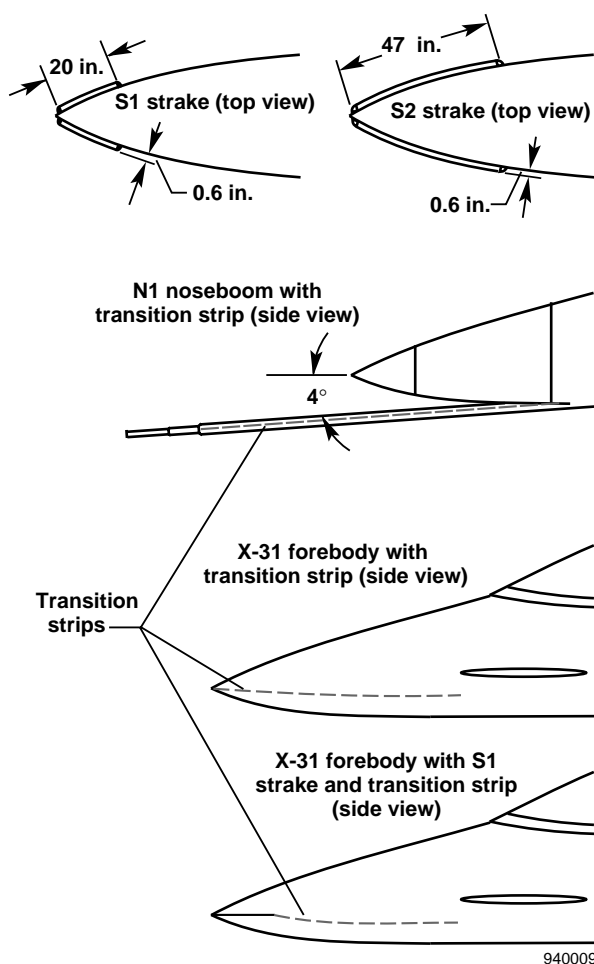


Figure 8. Strakes and boundary-layer transition strips (noseboom was present for all flight data).

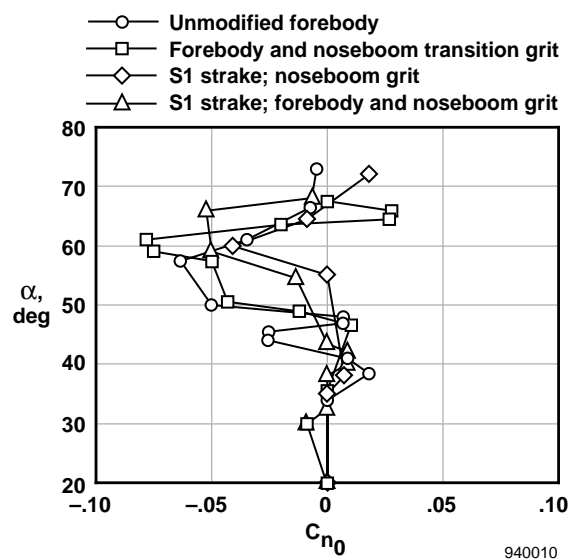


Figure 9. Yawing moment asymmetry as a function of angle of attack for 1-g maneuvers, ship 1.

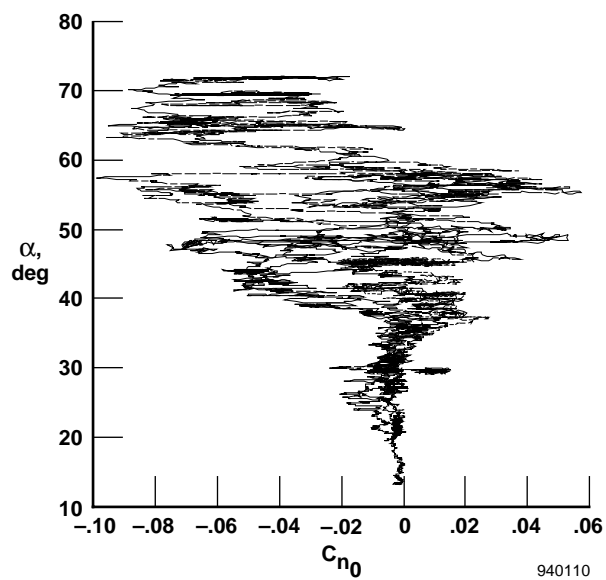


Figure 10. Yawing moment asymmetry as a function of angle of attack for 1-g maneuvers, ship 2 with an unmodified forebody.

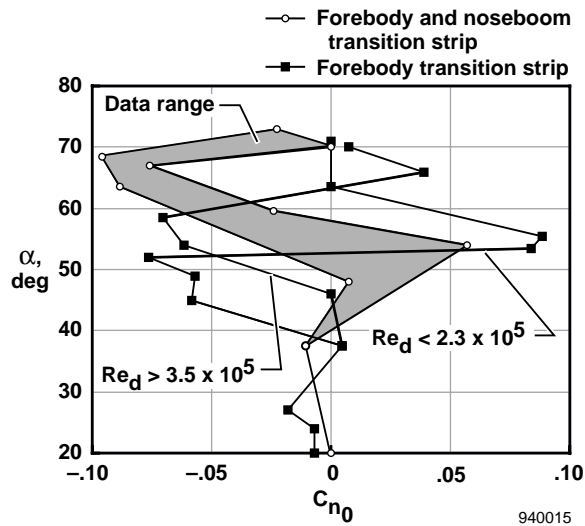


Figure 11. Yawing moment asymmetry as a function of angle of attack for 1-g maneuvers, ship 2 with transition strips.

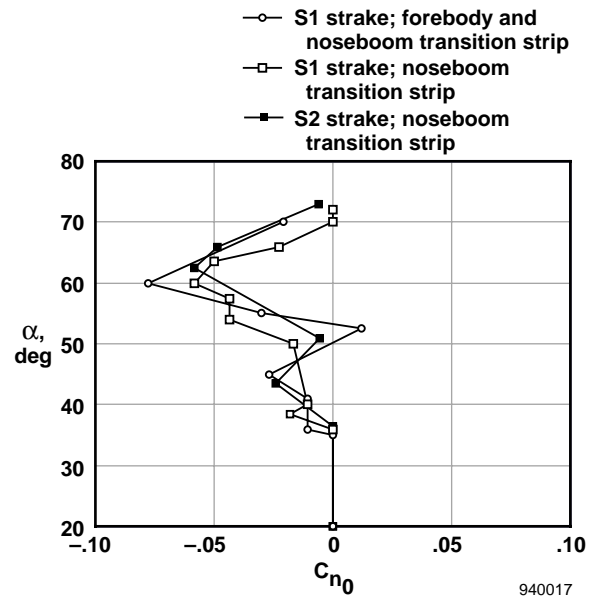


Figure 13. Yawing moment asymmetry as a function of angle of attack for 1-g maneuvers, ship 2 with strakes.

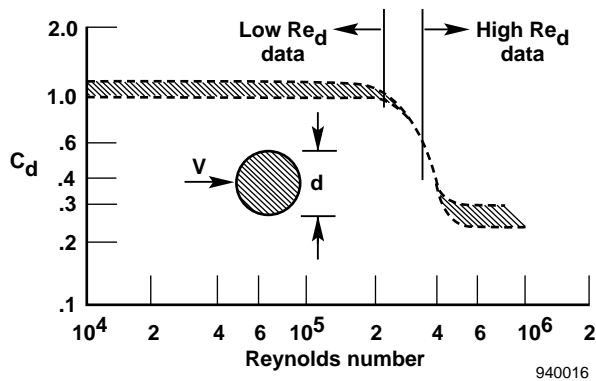


Figure 12. Variation of drag coefficient with Reynolds number for a circular cylinder.²³

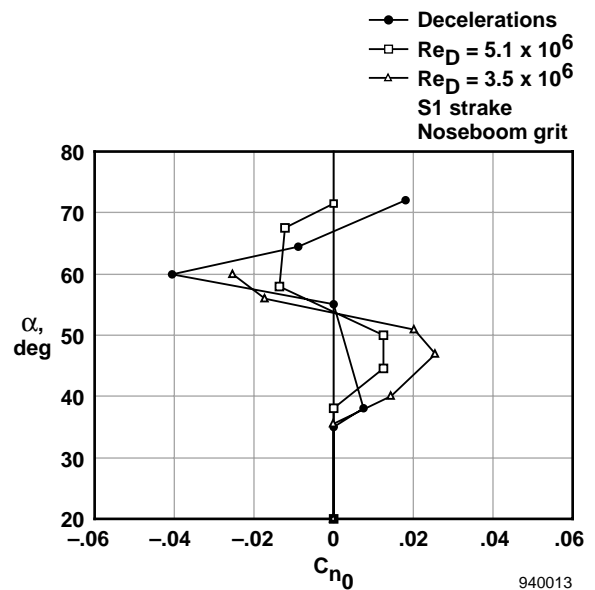


Figure 14. Yawing moment asymmetry as a function of angle of attack for dynamic maneuvers, ship 1 with S1 strakes and noseboom transition strips.

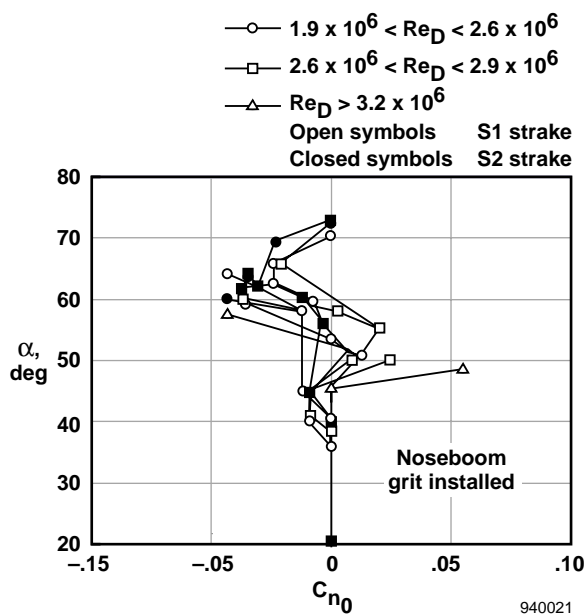


Figure 15. Yawing moment asymmetry as a function of angle of attack for dynamic maneuvers, ship 2 with strakes and noseboom transition strips.

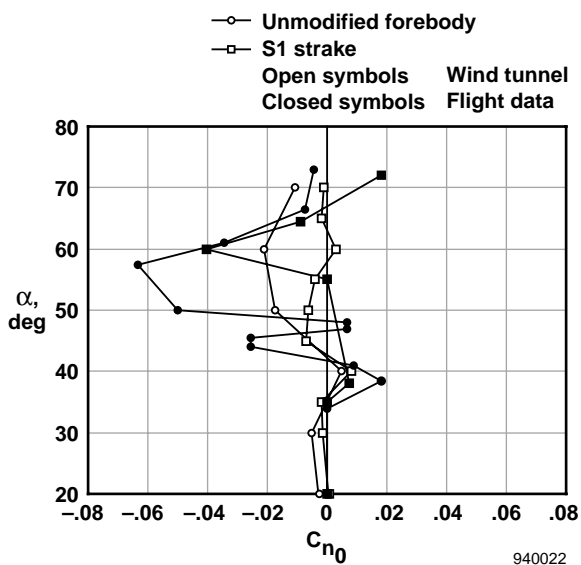


Figure 16. Comparison of wind-tunnel data to ship 1 flight results.

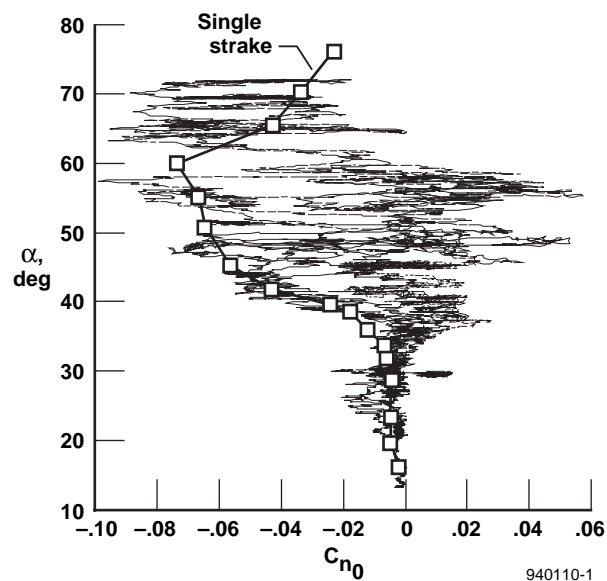
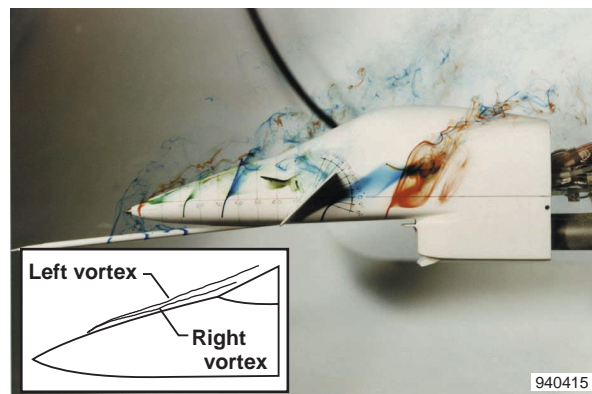
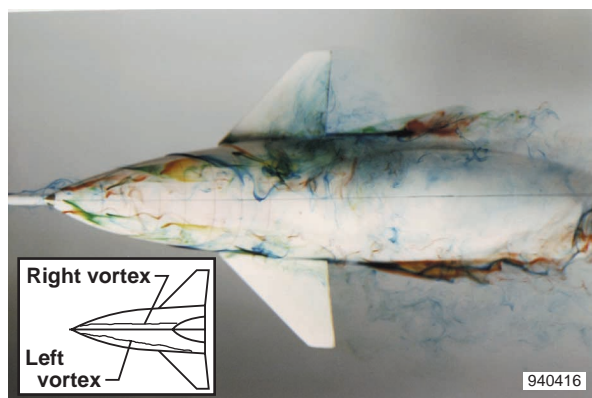


Figure 17. Comparison of ship 2 yawing moment asymmetry with wind-tunnel data (with the one-sided strake installed).



a) Side view.



b) Top view.

Figure 18. Water-tunnel visualization of the unmodified forebody at 60° angle of attack.

Paper: 42

Author: Mr. Cobleigh

Question by Mr. Cunningham: I have observed considerable pitch-rate effects on lateral-directional instabilities at high angle of attack. Do you have quantifiable data for the effects of pitch rate?

Answer: We had a significant number of rapid pitch maneuvers stopping at 30°, 40°, 50°, 60° or 70° angle of attack. The data showed that the asymmetry magnitude was less than the 1-g magnitudes in all cases. Once the pitching stopped, however, the asymmetry increased out to the nominal 1-g magnitude. Therefore, 1-g asymmetries were the worst case.

Question by Mr. Mendenhall: Some calculations of shed vorticity on X-31 during 0°-70° pitch up showed possible vortex impact on rudder at $\alpha \sim 45^\circ$. Was this seen in flow visualization?

Answer: No. Earlier water tunnel tests showed that the vortices broke down near the canard at very high angles of attack.

Question by Dr. Bredif: What is the influence of the strakes on the aerodynamic characteristics in the pitching plane?

Answer: The strakes guarantee that the boundary layer separation is symmetrical on each side of the forebody. Since the yawing moment is primarily caused by the boundary layer state (separated or attached), the yawing asymmetry is reduced. Since we are fixing separation, it should not matter how wide the strakes are. The strakes should also increase the vorticity in the vortex, but there is no evidence on whether this will help or hurt the vortex asymmetry.

Question by Dr. Greenwell: Was there much model vibration (in yaw) in the 30' x 60' Tunnel? (One possible cause of reduced *time*-averaged symmetry could be yaw/model coupling causing oscillatory asymmetry.)

Answer: I do not recall any model vibration. The system had a fairly rigid mount.